High diversity of Proteobacteria amid the dominance of a few Aquificae species in the vent-water of a Trans-Himalayan sulfur-borax hot spring

Nibendu Mondal[1,$], Subhajit Dutta[1], Sumit Chatterjee[1], Jagannath Sarkar[1], Mahamadul Mondal[1], Chayan Roy[2], Ranadhir Chakraborty[3] and Wriddhiman Ghosh[1,*]

Author Addresses:

[1] Department of Biological Sciences, Bose Institute, Kolkata, India

[2] Department of Plant and Environmental Sciences, University of Copenhagen, Copenhagen, Denmark

[3] Department of Biotechnology, University of North Bengal, Siliguri, India

Present Address:

[$] Division of Molecular Biology and Genomics, International Institute of Innovation and Technology, Kolkata, India

* **Correspondence:** Wriddhiman Ghosh (wriman@jcbose.ac.in / Wriman@rediffmail.com)

Keywords: Trans-Himalayan sulfur-borax hot springs, vent-water microbiome, hot spring mesophiles, Proteobacteria, Aquificae, antibiosis and virulence

---

Abstract

Little is known about the relative abundance and metabolisms of microorganisms present in the vent-waters of Trans-Himalayan hot springs. This study revealed a Bacteria-dominated microbiome in the ~84°C vent-water (microbial cell density ~8.5 × 10^4 mL^{-1}; live:dead cell ratio 17:10) of a sulfur-borax spring called Lotus Pond, situated at 4436 m, in Puga Valley. Aquificae accounted for 80% of all 16S rRNA-encoding reads within the metagenomic dataset, while only 14% of such reads were attributed to Proteobacteria. Post assembly, only 25% of all protein-coding genes identified were attributable to Aquificae, and ~41% to Proteobacteria. Annotation of raw metagenomic reads encoding 16S rRNAs, and/or PCR-amplified 16S rRNA genes, identified 163 bacterial genera, out of which 66 had been detected in past investigations of Lotus Pond's vent-water via 16S amplicon sequencing. Among these 66, *Fervidobacterium*, *Halomonas*, *Hydrogenobacter*, *Paracoccus*, *Sulfurihydrogenibium*, *Tepidimonas*, *Thermus* and *Thiofaba* (or their close phylogenomic relatives) were presently detected as metagenome-assembled genomes (MAGs). Remarkably, the MAG related to *Hydrogenobacter* alone accounted for ~56% of the entire metagenome, even as literature survey showed that only 15 out of the 66 genera consistently present in Lotus Pond have strains growing in the laboratory at >45°C, reflecting the continued existence of diverse mesophiles in the habitat. Most genes annotated within the MAGs/assembled-metagenome rendered bioenergetic functions (especially oxidative phosphorylation and rTCA/TCA cycles), while many (especially from Aquificae) conferred virulence functions

and antibiotics synthesis/resistance. These could help the Aquificae outcompete other native thermophiles, and contain the proliferation of the bacterial mesophiles that infiltrate the ecosystem.

Introduction

Hydrothermal environments, considered to be the nurseries of early life on Earth [1-3], are characterized by the entropic disordering of biomacromolecular systems, which in turn restricts their habitability [4, 5]. Thermophilic and hyperthermophilic microorganisms [6] are the habitual natives of hydrothermal vents, and for most taxa abundant at the 30-40°C sites of these ecosystems, habitability is progressively constrained in the 50°C to 100°C trajectory [5, 7-10]. Conversely, as the thermodynamic/bioenergetic cost of cell system maintenance get relaxed down the temperature gradient, habitability, and therefore *in situ* diversity, increases for most microbial taxa [11, 12].

Idiosyncratic to the above community structure axiomatic for hydrothermal ecosystems, a geochemically unusual category of Trans-Himalayan hot springs (poor in total dissolved solids including silicon, but rich in boron, sodium and diverse sulfur species), located on the either side of the tectonically active Indus Tsangpo Suture Zone (ITSZ, the collision intersection between the Asian and Indian continental crusts engaged in Himalayan orogeny) in eastern Ladakh, India [13-16], have been reported to feature extra-ordinarily high habitability [5, 10, 17, 18]. Concurrent to such reports of exceedingly bio-diverse microbiomes from the springs of the Puga and Chumathang geothermal areas situated in the south and north of the ITSZ respectively, studies of microbial diversity within the vent-waters, and vent-adjacent niches, of a number of hot springs located across discrete Himalayan and Trans-Himalayan geothermal regions have corroborated that hydrothermal environments were not “Thermophiles Only Territories” [19-25].

As for the well-studied Puga hydrothermal system, PCR-amplified 16S rRNA gene sequence-based investigations of microbial communities within the boiling vent-waters of a number of springs have revealed the presence of several such genera whose members are incapable of laboratory-growth at >45°C [10, 17, 18]. Diurnal fluctuations in the biodiversity and chemistry of the vent-waters, in conjunction with circumstantial geological evidences, indicated that the copious tectonic faults of this ITSZ-adjoining area serve as potential conduits for the infiltration of meteoritic water, and therewith mesophilic microorganisms, to the shallow geothermal reservoir [10]. Furthermore, shotgun metagenome sequencing-based investigation of microbial mat communities along the spring-water transit/dissipation channels of a hydrothermal microbialite of Puga has identified several genus-level populations to occupy such sites within the hydrothermal gradients which have temperatures tens of degree-Celsius above the *in vitro* growth-limits of those taxa [5, 26]. While the overall geomicrobiology of the Puga hot springs indicated the system’s peculiar chemistry (mineralogy) to be the key facilitator of the high habitability of the environment [5, 18], physiological attributes of a vent-water

isolate identified dissolved solutes such as lithium and boron, characteristic to the Puga hydrothermal system [15, 16], as the key enablers of high temperature endurance by the mesophilic bacteria present *in situ* [27].

Despite a considerable progress in our understanding of the geobiology of Trans-Himalayan sulfur-borax springs, we still do not have any quantitative idea about the composition of the vent-water microbiomes of these astrobiologically significant hydrothermal systems [16, 28, 29]. Although we have a fair measure of the microbial diversity in terms of the variety of taxa present, we are completely unaware of the relative abundance of the individual taxa constituting the microbiome. We also know nothing about the community metabolisms that enable ecosystem functioning in these boiling waters, except for the potential chemolithotrophic activities apparent from the presence of genera having known sulfur-oxidizing members, and the spatial abundance and isotope ratios of redox sulfur species [10]. To address these shortcomings in our knowledge on the ecology of Trans-Himalayan sulfur–borax spring systems, this study comprehensively reveals the vent-water microbiome of the Lotus Pond hot spring, which is one of the most conspicuous hydrothermal manifestations within the Puga valley [10, 16, 17]. While the bacterial diversity of Lotus Pond's vent-water has been investigated previously by means of 16S amplicon sequencing [10, 17], the present exploration, for the first time, unravelled the qualitative as well as quantitative architecture of the microbiome via whole metagenome shotgun sequencing, and fluorescence microscopy. Besides elucidating the dominance and equitability of taxa within the microbiome, the >15 giga base metagenomic sequence data generated was analyzed functionally to illuminate the cardinal aspects of community metabolism. Furthermore, PCR-amplified 16S rRNA gene sequencing and analysis was performed again on the current sample to evaluate the consistency of the taxonomic diversity of Lotus Pond's vent-water.

Results

Density of microbial cells in Lotus Pond

Gross density of microbial cells in the vent-water of Lotus Pond was found to approximately 8.5×10^4 mL^{-1}, via staining with 4′6-diamidino-2-phenylindole (DAPI), followed by hemocytometry using a fluorescence microscope (Fig. 1). On the other hand, the density of metabolically viable cells was estimated to be approximately 5.4×10^4 mL^{-1}, via staining with fluorescein diacetate (FDA), while that of apparently dead cells was 3.2×10^4 cells mL^{-1}, according to hemocytometry via propidium iodide (PI) staining. Thus, the ratio between the densities of metabolically active and dead cells in Lotus Pond's vent water was almost 1.7.

Microbiome structure reconstructed from assembled metagenome

Quality filtration of the native metagenomic sequence dataset having 31353866 read-pairs resulted in the retention of 31342225 read-pairs. Assembly of the quality-filtered dataset yielded 286918 contigs having a minimum and an average length of 200 and 563 nucleotides respectively (96% of all quality-filtered reads

participated in the assembly, at an average coverage of ~85X). While the largest contig obtained was 197270-nucleotide long, the consensus sequence of the assembled metagenome was ~162 million nucleotides, with a total of 379412, complete or partial, putative open reading frames (ORFs) or genes identified therein. Out of the 379412 ORFs identified, 220687 could be annotated as protein coding sequences (CDSs), of which again 220635 could be ascribed to potential taxonomic sources (Table S1). Approximately 97.3%, 1%, 1.5% and 0.2% of the taxonomically classifiable CDSs belonged to Bacteria, Archaea Eukarya and Viruses respectively.

The bacterial CDSs predicted were distributed over 23 phyla, with most of them being affiliated to Proteobacteria, followed by Aquificae, Firmicutes, Deinococcus-Thermus, Cyanobacteria, Chloroflexi, Bacteroidetes, Thermotogae, Thermodesulfobacteria and Actinobacteria. 13 other (minor) phyla were represented sparsely in the CDS catalog (Tables S1 and S2; Fig. 2A).

The small archaeal genetic diversity was contributed by unclassified Crenarchaeota/Thermoproteota, followed by Euryarchaeota (Tables S1 and S2). Most of the putatively eukaryotic CDSs detected exhibited highest sequence similarities with homologs from Opisthokonta, affiliated to either Fungi or Metazoa (Table S1). The few viral CDSs detected were mostly contributed by Podoviridae, Myoviridae, Siphoviridae and Caudovirales (Table S1).

Microbiome functions reconstructed from the assembled metagenome

210761 CDSs (Table S1) were ascribable to clusters of orthologous genes (COGs) that again were distributed across 23 categories (Table S6). Of these, Energy production and conversion, and DNA metabolism, had the maximum number of CDSs. Next in attendance were the COG categories Translation, ribosomal structure and biogenesis, Amino acid transport and metabolism, Cell wall/membrane/envelope biogenesis, Coenzyme transport and metabolism, and Inorganic ion transport and metabolism.

For energy production and conversion, maximum homologs were detected for NADH-quinone oxidoreductase subunit L and cytochrome c oxidase subunit I. Oxidative phosphorylation was the most represented pathway. Maximum CDSs were attributed to the biochemical modules NADH:quinone oxidoreductase, reductive citrate cycle, citrate cycle, and cytochrome c oxidase. Notably, reductive pentose phosphate cycle accounted for relatively fewer CDSs.

Regarding DNA metabolism, maximum homologs were detected for a putative transposase. Mismatch repair, homologous recombination, replication, and nucleotide excision repair were the most represented pathways. Maximum CDSs, were attributed to the module DNA polymerase III complex.

For translation and ribosomes, maximum homologs were detected for elongation factor Tu. Aminoacyl-tRNA biosynthesis was the most represented pathway. Ribosome was the maximally represented biochemical module.

Regarding amino acid transport and metabolism, maximum homologs were detected for glycine cleavage H protein and cysteine desulfurase. Biosynthesis of secondary metabolites was the most represented pathway. Maximum CDSs were attributed to the module photorespiration.

Regarding cell wall/membrane/envelope biogenesis, maximum homologs were detected for glutamine:fructose-6-phosphate isomerizing transaminase and GTP-binding LepA. Amino sugar and nucleotide sugar metabolism, antibiotics biosynthesis, and peptidoglycan biosynthesis were the most represented pathways. At the module level, nucleotide sugar biosynthesis, dTDP-L-rhamnose biosynthesis, lipoprotein-releasing system, lipopolysaccharide biosynthesis (KDO2-lipid A), multidrug resistance, efflux pumps AcrAB-TolC/SmeDEF, AcrAD-TolC, MexAB-OprM, and AmeABC were maximally represented.

For coenzyme transport and metabolism, maximum homologs were detected for uroporphyrin-III C-methyltransferase. Secondary metabolites biosynthesis, porphyrin metabolism, pantothenate and CoA biosynthesis, antibiotics biosynthesis, were the most represented pathways. Heme biosynthesis was the most represented module.

Regarding inorganic ion transport and metabolism, maximum homologs were detected for NADH-quinone oxidoreductase subunit L. ABC transporters, oxidative phosphorylation, quorum sensing, and two-component system, were the most represented pathways. At the module level, NADH:quinone oxidoreductase, peptides/nickel transport, phosphate transport, iron complex transport, nickel transport, NitT/TauT family transport, nitrate/nitrite transport, and Iron(III) transport, were represented maximally.

Genus-level constituents of the microbiome

Taxonomic classification of CDSs was not extended up to genus. Instead, generic components of the microbiome were delineated via taxonomic classification of (i) raw metagenomic reads corresponding to 16S rRNA genes, and (ii) OTUs clustered from PCR-amplified 16S rRNA gene sequences.

Out of the 62684450 quality-filtered metagenomic reads analyzed, 81686 represented parts of prokaryotic 16S rRNA genes: 81223 bacterial, 396 archaeal and 67 unclassifiable (Table S3). No read having meaningful sequence similarity with any eukaryotic 18S rRNA gene was detected.

The metagenomic reads corresponding to bacterial 16S rRNA genes were distributed over 12 phyla, of which Aquificae exhibited an overwhelming majority (Table S3; Fig. 2B). Substantive number of such reads were also ascribable to Proteobacteria, Deinococcus-Thermus and Firmicutes, while Thermodesulfobacteria, Cyanobacteria, Thermotogae, Bacteroidetes, Chloroflexi, Actinobacteria, Armatimonadetes / Armatimonadota and Synergistetes accounted for fewer reads. The proteobacterial reads, again, were mostly contributed by Gammaproteobacteria (Table S3; Fig. 2B). Out of the 81223 reads identified as parts of bacterial 16S rRNA genes, 70729 were classifiable under 92 genera led by *Hydrogenobacter*, *Sulfurihydrogenibium*, *Halomonas*, *Vibrio*, *Thermus*, *Tepidimonas* and *Paracoccus* (Table S3).

All metagenomic reads coresponding to archaeal 16S rRNA genes were attributable to Crenarchaeota, and very few were classifiable up to genus, detecting only *Aeropyrum*, *Stetteria* and *Pyrobaculum* (Table S3).

PCR-amplified 16S rRNA gene sequence analysis revealed 602 bacterial OTUs distributed over 16 phyla, of which Proteobacteria accounted for an overwhelming majority of OTUs (Table S4). 249 OTUs were classifiable upto genus, identifying 121 entities, of which *Vibrio*, *Halomonas* and *Thermus* accounted for most OTUs (Table S4). 16S amplicon sequencing also revealed 30 archaeal OTUs, of which, 10 were ascribable to Crenarchaeota, and 6 each to Euryarchaeota and Nitrososphaerota (Table S4). 10 OTUs were classifiable upto genus, identifying *Methanomassiliicoccus*, *Methanospirillum* and *Nitrososphaera* (Table S4).

Population genome bins from the assembled metagenome

Binning all metagenomic contigs ≥2500-nucleotide long, followed by refinement and optimization of the bins, yielded 14 bacterial (Tables 1 and S5; Fig. 3) and one archaeal (Tables 1 and S5) metagenome-assembled genomes (MAGs). All the MAGs except one had <5% contamination, while 9 out of the total 15 had >90% completeness, four possessed 50-82% completeness, and two were <50% complete. In terms of consensus sequence length, the MAGs classified as *Vibrio metschnikovii* and *Halomonas* sp. were the largest, while the one ascribed to unclassified Thermodesulfobacteriaceae was the smallest. Overall ~68% of all quality-filtered metagenomic reads-pairs available matched MAG sequences concordantly, with LotusPond_MAG_Unclassified_Aquificaceae alone accounting for ~56% read-pairs.

Apart from house-keeping genes, all the MAGs encompassed genes for heat stress management. Irrespective of their completeness level, MAGs affiliated to truly thermophilic taxa had less than 10 such genes each, whereas almost all the MAGs affiliated to mesophilic taxa had ≥10 heat stress management genes each. Almost all the MAGs contained genes for managing oxidative and periplasmic stress; a half of them had genes for withstanding carbon starvation and nitrosative stress. Eight MAGs encoded genes conferring high frequency of lysogeny as a means of stress response. Every bacterial MAG, but not the archaeal one, encompassed genes for stringent response to environmental stimuli via (p)ppGpp metabolism. Most of the MAGs encoded versatile sporulation-associated proteins, while those affiliated to mesophilic or moderately thermophilic taxa encoded a universal stress protein.

All but one MAG contained genes for cation transport; most had genes for twin-arginine motif-based protein translocation and Ton and Tol transport systems, while some encoded ABC transporters, Uni- Sym- and Antiporters, TRAP transporters, and various secretion systems. Half of the MAGs harbored genes for flagellar motility or chemotaxis; protection against metals, toxins, and antibiotics; and CRISPR systems.

Details of the phylogenomic relationships, and adaptationally useful genes, of the MAGs are given in Supplementary Results.

Discussion

Comparing microbial diversities revealed by shotgun metagenomics and 16S amplicon sequencing

Two archaeal phyla, Crenarchaeota and Euryarchaeota, were identified by taxonomic annotation of CDSs (Table S2), but searching of raw metagenomic reads for 16S rRNA-coding sequences detected only Crenarchaeota, while 16S amplicon sequencing identified Crenarchaeota, Euryarchaeota and Nitrososphaerota. *Aeropyrum*, *Pyrobaculum* and *Stetteria*, identified by direct annotation of metagenomic reads went undetected in 16S amplicon-based analysis, whereas *Methanomassiliicoccus*, *Methanospirillum* and *Nitrososphaera*, detected via 16S amplicon sequencing, were undetectable in direct read-annotation (Tables S3 and S4).

For Bacteria, 23 phyla were identified via taxonomic classification of CDSs: of these, 10 were major phyla embracing >2000 CDSs each and 13 were minor phyla with <500 CDSs each (Table S2; Fig. 2A). Annotation of raw metagenomic reads detected 12 phyla, including the 10 major ones mentioned above, plus one of the 13 minors (Synergistetes), and a new phylum (Armatimonadetes) that was not represented in the CDS catalog (Table S3; Fig. 2B). 16S amplicon-based OTU analysis identified 16 phyla, including the 10 majors identified from CDS annotation, plus two of the 13 minor phyla (Acidobacteria and Synergistetes), and Armatimonadetes, and three new phyla (Dictyoglomi, Rhodothermaeota and Spirochaetes) that were not represented among the CDSs or the raw reads encoding 16S rRNAs (Table S4).

Annotation of raw metagenomic reads revealed 92 bacterial genera, while OTU analysis identified 121. Between these two sets, 50 genera were common (Tables S3 and S4), of which seven (*Fervidobacterium*, *Halomonas*, *Paracoccus*, *Sulfurihydrogenibium*, *Tepidimonas*, *Thermus* and *Vibrio*) were represented as MAGs, and two (*Hydrogenobacter* and *Thiofaba*) were represented by very closely related MAGs (LotusPond_MAG_Unclassified_Aquificaceae and LotusPond_MAG_Unclassified_Chromatiales; Supplementary Results). Of all the genera represented among the MAGs (Tables 1 and S5; Fig. 3), *Thermosynechococcus* alone was not detected in any 16S rRNA gene sequence-based analysis; however, LotusPond_MAG_Thermosynechococcus_sp. did encompass a near-complete 16S rRNA gene, 99.6% similar to the *Thermosynechococcus elongatus* BP-1 homolog.

A number of studies have found 16S amplicon sequencing to underrepresent taxa at different hierarchical levels [30-33], whiereas others have reported similar outcomes with shotgun metagenome sequencing [34, 35]. The present data demonstrated that annotation of raw metagenomic reads corresponding to 16S rRNA genes reliably delineated bulk of the diversity at both phylum and genus levels, whereas CDSs detected within the assembled metagenome (or for that matter, 16S amplicon sequences) revealed the less-abundant taxa more effectively.

Lotus Pond's vent-water microbiome remains stable over time

Lotus Pond has been explored for its vent-water bacterial (but not archaeal) diversity, via 16S amplicon sequencing alone, on five previous time-points [10, 17]. A comparison of the present 16S amplicon-based data with those from the past showed that all the 16 bacterial phyla detected in the current investigation (Table S4), except Rhodothermaeota and Synergistetes, had been identified in previous exploration(s). The five previous explorations too had collectively discovered 16 phyla, of which only Ignavibacteriae and Nitrospirae went undetected in the present 16S amplicon-based survey. Furthermore, Actinobacteria, Aquificae, Bacteroidetes, Chloroflexi, Cyanobacteria, Deinococcus-Thermus, Firmicutes, Proteobacteria, Synergistetes, Thermodesulfobacteria and Thermotogae were consistently detected in the present annotation of CDSs, 16S rRNA-encoding metagenomic reads, and OTUs clustered from 16S amplicon sequences. All these, except Synergistetes, were also detected in previous investigations.

At the genus level, 121 entities were detected in the current PCR-based investigation, out of which 59 (Table S4) were identified in one or more previous explorations, which in turn had collectively discovered 156 genera. Seven out of the 97 genera that were identified previously, but not in the present PCR-based analysis, got identified in the annotation of raw metagenomic reads corresponding to 16S rRNA genes (Table S3). In this way, a total of 66 bacterial genera (Table 2) were found to be present regularly in Lotus Pond's vent-water over a period of approximately ten years. Notably, eight out of these 66 genera (*Fervidobacterium*, *Halomonas*, *Hydrogenobacter*, *Paracoccus*, *Sulfurihydrogenibium*, *Tepidimonas*, *Thermus* and *Thiofaba*), or their very close phylogenomic relatives, were detected as MAGs in the present investigation (Supplementary Results; Table S5).

Lotus Pond is not reserved for thermophiles, albeit Aquificales predominate numerally

29 out of the 92 bacterial genera identifed via annotation of raw metagenomic reads encompass strains having laboratory-growth above 45°C (Table S3). Likewise, only 30 out of the 121 genera detected via 16S amplicon sequencing have strains with laboratory-growth above 45°C (Table S4). Among the 66 bacterial genera present regularly in the vent-water, only 15 have strains with laboratory-growth above 45°C (Table 2). Corroborative to this high diversity of bacterial mesophiles, 41.2% of all taxonomically classifiable CDSs were ascribable to Proteobacteria, whereas only 24.5% were affiliated to Aquificae (Table S2; Fig. 2A).

Although phylogenetic relatives of mesophilic bacteria overwhelm the alpha diversity of Lotus Pond, thermophilic Aquificales dominate in terms of relative abundance. Only two MAGs related to unclassified Aquificaceae or *Hydrogenobacter* (laboratory-growth maxima: 85°C [36]) and *Sulfurihydrogenibium* (laboratory-growth maxima: 80°C [37]) collectively made up 59.4% of the whole metagenome (Table S5), and ~80% of all 16S rRNA-encoding metagenomic reads (Table S3).

Among the other taxa identified as MAGs, *Fervidobacterium* (laboratory-growth maxima: 90°C [38]), *Thermus* (laboratory-growth maxima: 80°C [39]), Thermodesulfobacteriaceae (laboratory-growth maxima:

100°C [40]), and Desulfurococcales (laboratory-growth maxima: 110°C [41]) have strains growing at temperatures above or within the ten-year range (78-85°C) recorded for Lotus Pond's vent-water [10, 16, 17]. These MAGs together accounted for ~3% of the metagenome.

Cyanobacteria have been found in 73-85°C springs [42, 43], but *Thermosynechococcus* are restricted to ≤70°C waters [44, 45] and its cultured strains grow at ≤60°C [46, 47]. *Halomonas* [48], *Paracoccus* [27, 49], *Thiofaba* [50], *Tepidimonas* [51] and *Vibrio* [52] have laboratory-growth maxima of 50°C, 45°C (or 50°C under special conditions), 51°C, 60°C and 50°C respectively. Thus, eight out of the 15 Lotus Pond MAGs, collectively accounting for 5.6% of the metagenome, were affiliated to genera encompassing strains that grow only at temperatures below the range known for Lotus Pond's vent-water. That said, *Halomonas*, *Paracoccus*, *Tepidimonas*, *Thiofaba* and *Vibrio* have been isolated from hydrothermal vents or vent-adjacent environments, and found to exhibit varying degrees of thermal endurance [27, 50, 51, 53-55].

Genomic resources that can help mesophiles survive in the Lotus Pond habitat

Lotus Pond's assembled metagenome encompassed several such genes that could be potentially decisive in thermal adaptation, especially in the context of the vent-water's geochemistry and the spring's topography. A majority of these CDSs were ascribable to phylogenetic relatives of mesophilic bacteria, and their examples included genes encoding heat shock proteins, molecular chaperones/chaperonins, universal stress proteins, methionine sulfoxide reductases, peroxide-reducing enzymes, and diverse proteins adapted structurally/functionally to high heavy metal concentrations. While copious fatty acid desaturase homologs encoded by the metagenome may help increase the rigidity of cell membranes (via unsaturation of fatty acids), numerous genes available for flagellar structure/function, chemotaxis, cell adhesion/aggregation, biofilm formation, and quorum sensing might assist microorganisms position themselves at biophysically/biochemically best-suited sites along the hydrothermal gradients occurring in the vent (Lotus Pond) to river (Rulang) trajectory. Furthermore, Lotus Pond's metagenome contained several genes encoding proteins that control/modulate/inhibit DNA gyrase activity. In true thermophiles, reverse gyrases (RGs) are indispensible as they render positive supercoils in the DNA to counter-balance the negative supercoils promoted by gyrases, and *in situ* heat [56]. RGs also help avert incorrect aggregation of denatured DNA, and facilitate correct annealing [57]. Expectedly, Lotus Pond MAGs affiliated to Aquificaceae, Desulfurococcales, *Fervidobacterium* and *Sulfurihydrogenibium* encoded RGs, but those belonging to phylogenetic relatives of mesophilic or moderately thermophilic bacteria did not. Nevertheless, MAGs affiliated to *Halomonas*, *Vibrio*, *Tepidimonas* and *Paracoccus* did encode gyrase inhibitors/modulators such as YacG/PmbA/TldD which are known to nullify gyrase activity [58, 59]; notably, several homologs of these genes ascribable to other mesophilic taxa were also present in the assembled metagenome. Future studies of metatranscriptomics and metaproteomics are needed alongside multi-omic investigations of pure culture

isolates to ascertain whether and how the above specialties help hot spring mesophiles endure high temperatures over time and space.

Why are virulence genes abundant in Lotus Pond?

The Lotus Pond metagenome encompassed hundreds of genes for hemagglutinin and hemolysin biosynthesis, and stationary phase metabolisms including the formation of persister cells (Table S1). While haemolysins may have roles in osmoregulation and extreme-temperature response [60], formation of persister cells can help bacterial mesophiles attain ultra-slow metabolic states central to thermal endurance [27]. Furthermore, the metagenome encompassed more than a thousand genes (Supplementary Results) for constructing Type-I through Type-IX secretion systems (SSs), excepting Type-V and Type-VII. While all these SSs have documented roles in bacterial survival within eukaryotic hosts, their ecological roles are also not unappreciated [54]. For instance, macromolecules moved across the cell membrane by Type-II SS often serve as local and long-range effectors of nutrient acquisition and biofilm formation under adverse conditions [61]. Type-III SSs can promote response to high salts and peroxides [62], besides potentially interacting with Type-IV SSs to mitigate different environmental stressors [63]. Type-IV may also kill other bacteria to eliminate competition in nutrient-deprived habitats [64]. Type-VI SSs regulate quorum sensing with wide-ranging adaptational implications [65]. Type-VIII SS is implicated in adhesion, aggregation, and biofilm formation [66], while Type-IX confers gliding motility [67], so they may be instrumental in placing microorganisms at biophysically endurable sites within the hydrothermal gradients.

Antibiosis as an instrument of ecosystem domination

Abundance of antibiotic synthesis (ASGs) and resistance (ARGs) genes in hydrothermal environments is a topic of considerable contemporary interest, and many thermophilic bacteria have been reported to produce antibiotics, which in turn can generate and spread resistance in the ecosystem [68]. Lotus Pond's metagenome contained thousands of genes for the biosynthesis of monobactam, streptomycin, prodigiosin, acarbose/validamycin, novobiocin, vancomycin, phenazine, carbapenem, penicillin/cephalosporin, neomycin/kanamycin/gentamicin, staurosporine and enediyne; and resistance of beta-lactams, vancomycin and cationic antimicrobial peptides (Supplementary Results).

~50% of the ASGs detected were ascribable to the few thermophilic/hyperthermophilic taxa present in the microbiome (Aquificae, Thermodesulfobacteria, Deinococcus-Thermus, Euryarchaeota and Crenarchaeota), while the large diversity of mesophilic taxa (including the moderate thermophiles) accounted for the remaining 50%.

The thermophilic/hyperthermophilic taxa present were not so enriched in ARG diversity as they were for ASGs, and account for ~25% of all ARGs detected. Crenarchaeota and Euryarchaeota were not represented in the ARG catalog at all, while ARG diversities for Aquificae, Deinococcus-Thermus and

Thermodesulfobacteria were less than their own ASG diversities, as well as the ARG diversities embraced by the mesophilic and moderate thermophilic taxa. Furthermore, ARG diversities of the latter types of taxa were either more enriched than, or almost as rich as, their own ASG diversities.

The elaborate antibiosis machinery possessed by the few Aquificae species present in the microbiome seems to have helped them get rid of potential niche overlap with their ecological equivalents, the thermophilic/hyperthermophilic archaea. The latter groups, despite being equally/better equipped to manage thermal stress, were apparently consigned to the status of microscopic minorities within the community because they were far less armed with ASGs and practically defense-less against antibiotics. For the Lotus Pond Aquificae, antibiosis as a strategy of establishing ecological supremacy may not have been equally effective in decimating the high *in situ* diversities of the mesophilic to moderately thermophilic Proteobacteria, Firmicutes, Cyanobacteria, Chloroflexi and Bacteroidetes, and the thermophilic Deinococcus-Thermus, Thermotogae and Thermodesulfobacteria (as these taxa were well equipped with ASGs and ARGs), but the potent contrivances of biomolecular warfare that the Aquificae possessed must have exacerbated the latter groups' bioenergetic costs of thermal endurance. Consequentially, the few Aquificae species present in the Lotus Pond vent-water not only managed to critically restrict the proliferation of other bacterial thermophiles native to the habitat, but also keep a tab on the flux of the mesophilic bacteria that infiltrate the ecosystem.

Methods

Study site and sampling

Lotus Pond, located at 33°13'46.3"N and 78°21'19.7"E, is one of the most prominent hot springs or geysers within the Puga valley, which in turn is one of the most vigorous geothermal areas of the Indian Trans-Himalayas; notably Puga Valley is situated on the Changthang plateau of eastern Ladakh, at an altitude of 4436 m, where the boiling point of water remains at around 85°C [10, 16, 69]. The venting point is embedded in a hot water pool that has been formed by its own discharges and lies within the old crater formed from the same hydrothermal eruption that gave rise to the geyser itself. From one side of the hot water pool, the spring-water flows over thin unstable terraces of geothermal sinters, into the Rulang rivulet, which meanders through the valley of Puga. On the other flank of the hot water pool, a wall of travertine, sulfur, and boron mineral deposits guard the crater and debars the spring-water from escaping the pool [10, 16].

Water (temperature 84°C, pH 7.5) was collected from Lotus Pond's vent at 13:00 h of 29 October 2021, when ebullition was strong and fumarolic activity copious. For microscopic studies, 500 mL water was passed through a sterile 0.22 µm mixed cellulose ester membrane filter (Merck Life Science Private Limited, India) having a diameter of 47 mm, and inserted into a cryovial containing 0.9% (w/v) NaCl solution supplemented with 15% (v/v) glycerol. Simultaneously, for the extraction of total environmental DNA (metagenome), a total of 5 L water was passed through five individual sterile 0.22 µm filters, each of which was inserted into a

cryovial containing 5 mL of 50 mM Tris:EDTA (pH 7.8). All the cryovials were sealed with parafilm (Tarsons Products Limited, India), packed in polyethylene bags, put into dry ice, and air lifted to the laboratory at Bose Institute in Kolkata.

Enumeration of microbial cells

Total microbial cell count per unit volume of vent-water was determined alongside the number of viable and non-viable cells present. The microbial cells that were filtered out from 500 mL vent-water were first detached from the adherence matrix by shredding the filter with sterile scissors, and then vortexing for 30 min, within the NaCl-glycerol containing cryovial in which the filter was inserted on field. The vial was spun at 1000 *g* for 5 seconds to allow the filter shreds to settle down. Finally, the supernatant was collected (without disturbing the bottom debris), its exact volume measured, and then analyzed as described previously [70] using a hemocytometer (Paul Marienfeld GmbH & Co. KG, Germany) and an upright fluorescence microscope (Olympus BX53 Digital, Olympus Corporation, Japan), with the axiom that it contained all the microbial cells that were present in the 500 mL vent-water filtered on field. The cell suspension was stained with DAPI, FDA or PI solution, and cell numbers were counted as described previously [71].

Metagenomics

Metagenome was extracted from the microbial cells that were filtered out from Lotus Pond's vent-water in 0.22 µm mixed cellulose ester membrane filter, as described previously [5, 10, 18]. Paired end (2 × 250 nucleotides) whole metagenome shotgun sequencing was performed on Novaseq 6000 platform (Illumina Inc., USA). Clipping of adapters and quality-filtering of the trimmed sequences (for average Phred score ≥20) were carried out using Trim Galore v0.6.4. *De novo* assembly of the metagenomic sequence was performed using Megahit v1.2.9 [72]. ORFs were first identified within the assembled contigs using Prodigal v2.6.3 [73], and then annotated as potential CDSs by searching against the eggNOG database v5.0 [74] using eggNOG-mapper v2.1.9 [75].

Quality-filtered raw reads were searched against the RDP rrnDB database v5.8 [76] to extract sequences matching prokaryotic 16S rRNA genes, using Bowtie2 v2.2.5 [77]. The extracted reads were annotated taxonomically using RDP Classifier (http://rdp.cme.msu.edu/classifier/classifier.jsp). The quality-filtered read-set was also searched against the SILVA database v138.1 [78] to extract sequences matching eukaryotic 18S rRNA genes, using the Basic Rapid Ribosomal RNA Predictor tool Barrnap v0.9 [79]. The extracted reads were annotated taxonomically using Silva Alignment, Classification and Tree Service [80].

Construction of MAGs

Metagenomic contigs were first binned into putative population genomes or MAGs using Metabat2 v2.12.1 [81], MaxBin2 v2.2.4 [82], and CONCOCT v1.1.0 [83]. Best quality MAGs were then selected using DASTool v1.1.6 [84] and checked for their completeness and contamination levels using CheckM v1.2.2 [85].

Taxonomic identity of the selected MAGs was first predicted independently via searches for genom-genome relatedness conducted using Genome Taxonomy Database Toolkit (GTDB-Tk) v1.7.0 [86], Rapid Annotations using Subsystems Technology (RAST) [87], and Type Strain Genome Server (TYGS) in default mode [88]. As and when required, MAG versus genome/MAG pairs were tested for dDDH using the Genome-to-Genome Distance Calculator v3.0 [88]. Orthologous genes-based average nucleotide identity (ANI) between a pair of MAG and genome/MAG was calculated using ChunLab's online ANI Calculator [89]. All MAGs were annotated using Prokaryotic Genome Annotation Pipeline (https://www.ncbi.nlm.nih.gov/genome/annotation_prok/), and phylogeny of bacterial MAGs, in relation to their closest genomic relatives, was reconstructed based on conserved marker gene sequences, using the Up-to-date Bacterial Core Gene Pipeline v3.0 [90]. The best fit nucleotide substitution model was selected using ModelTest-NG v0.1.7 [91], following which a maximum likelihood tree was generated using RAxML v8.2.12 [92]. The Interactive Tree of Life v6.7.5 [93] was used to visualize the phylogram. Relative abundance of the individual MAGs within the metagenome was determined by mapping raw read-pairs onto the different MAG sequences using Bowtie2.

16S amplicon sequencing and analysis

PCR-amplified 16S rRNA gene sequence-based taxonomic diversity was revealed using the fusion primer protocol [10, 17, 94] on the Ion S5 DNA sequencing platform (Thermo Fisher Scientific, USA), which in turn involved PCR amplification and sequencing of the V3 regions of all Bacteria-specific 16S rRNA genes and V4-V5 regions of all Archaea-specific 16S rRNA genes [18] present in the Lotus Pond metagenome. Reads present in an amplicon sequence dataset (725025 and 589009 reads were there in the bacterial and archaeal sets respectively) were trimmed for their adapters, filtered for average Phred score ≥20 and length >100 nucleotides, and then clustered into operational taxonomic units (OTUs) by Usearch v10.0.259 [95]. While singleton sequences were eliminated before clustering, OTUs generated were classified taxonomically based on their consensus sequences using the RDP Classifier. Rarefaction curves (Fig. S1) were generated via Usearch.

Details of microscopy and microbiome analyses are given in Supplementary Methods.

Data availability

The whole metagenome shotgun sequence dataset was submitted to the Sequence Read Archive (SRA) of the National Center for Biotechnology Information (NCBI), USA, under the BioProject PRJNA296849, with the BioSample and Run accession numbers SAMN31749247 and SRR22364517 respectively. The bacterial and archaeal 16S amplicon sequence datasets were submitted to the SRA, under the BioProject PRJNA296849, with BioSample accession numbers SAMN32724325 and SAMN32724260, and Run accession numbers SRR23072972 and SRR23072970, respectively.

Acknowledgements

This research was financed by Bose Institute (via intramural faculty grants) as well as the Science and Engineering Research Board (SERB), Government of India (GoI) (SERB grant number EMR/2016/002703). N.M. received fellowships from SERB and Bose Institute. S.D. and J.S. obtained their fellowships from Council of Scientific and Industrial Research, GoI. S.C. and M.M. received a fellowship from the Department of Biotechnology, GoI. We thank Professor Shubhra Ghosh Dastidar and Sri Sanjib Kumar Gupta for helping with computational resources.

Author contributions

W.G. conceived the program, designed the experiments, interpreted the results, and wrote the paper. N.M. anchored and harnessed all the modules of the study, performed the experiments of both microscopy and bioinformatics, and analyzed and curated the data. S.D., J.S. and C.R. performed bioinformatics studies, while S.C. and M.M. carried out microscopic studies. W.G., N.M., S.D. and S.C. also performed the field works. R.C. and C.R. made intellectual contributions to the overall work as well as the manuscript. All the authors read and vetted the paper.

Competing interests

The authors declare no competing interests.

Additional information

Supplementary information in the form of an MS Word file named “Supplementary_Information.doc”, and an MS Excel file named “Supplementary_Dataset.xlsx”, accompany this paper.

References

1. Wächtershäuser G. From volcanic origins of chemoautotrophic life to Bacteria, Archaea and Eukarya. Philos Trans R Soc B. 2006;361:1787-1808.

2. Patel BH, Percivalle C, Ritson DJ, Duffy CD, Sutherland JD. Common origins of RNA, protein and lipid precursors in a cyanosulfidic protometabolism. Nat Chem. 2015;7:301-307.

3. Ranjan S, Todd ZR, Sutherland JD, Sasselov DD. Sulfidic anion concentrations on early earth for surficial origins-of-life chemistry. Astrobiology. 2018;18:1023-1040.

4. Fields PA. Protein function at thermal extremes: balancing stability and flexibility. Comp Biochem Physiol A Mol Integr Physiol. 2001;129:417-431.

5. Roy C, Rameez MJ, Haldar PK, Peketi A, Mondal N, Bakshi U, et al. Microbiome and ecology of a hot spring-microbialite system on the Trans-Himalayan Plateau. Sci Rep. 2020;10:5917.

6. Kristjansson JK, Stetter KO. Thermophilic bacteria. In: Kristjansson JK, Stetter KO (eds). Thermophilic bacteria. 1st ed. CRC press, 2021. pp 1-18.

7. Hall JR, Mitchell KR, Jackson-Weaver O, Kooser AS, Cron BR, Crossey LJ, et al. Molecular characterization of the diversity and distribution of a thermal spring microbial community by using rRNA and metabolic genes. Appl Environ Microbiol. 2008;74:4910-4922.

8. Everroad RC, Otaki H, Matsuura K, Haruta S. Diversification of bacterial community composition along a temperature gradient at a thermal spring. Microbes Environ. 2012;27:374-381.

9. Tang J, Liang Y, Jiang D, Li L, Luo Y, Shah MM, et al. Temperature-controlled thermophilic bacterial communities in hot springs of western Sichuan, China. BMC Microbiol. 2018;18:134.

10. Roy C, Mondal N, Peketi A, Fernandes S, Mapder T, Volvoikar SP, et al. Geomicrobial dynamics of Trans-Himalayan sulfur–borax spring system reveals mesophilic bacteria's resilience to high heat. J Earth Syst Sci. 2020;129:157.

11. Chiriac CM, Szekeres E, Rudi K, Baricz A, Hegedus A, Dragoş N, et al. Differences in temperature and water chemistry shape distinct diversity patterns in thermophilic microbial communities. Appl Environ Microbiol. 2017;83:e01363-17.

12. Ruhl IA, Sheremet A, Smirnova AV, Sharp CE, Grasby SE, Strous M, et al. Microbial functional diversity correlates with species diversity along a temperature gradient. Msystems. 2022;7:e00991-21.

13. Gansser A. Geology of the Himalayas. London: Interscience Publishers, 1964.

14. Garrett DE. Borates: Handbook of deposits, processing, properties, and use. Academic Press, 1998.

15. Rai AP. Compilation of data on chemical analysis of water and gas samples from North West Himalaya and adjoining areas. Bulletin Series-C, No. 5, Geological Survey of India, 2001.

16. Ghosh W, Mallick S, Haldar PK, Pal B, Maikap SC, Gupta SK. Molecular and cellular fossils of a mat-like microbial community in geothermal boratic sinters. Geomicrobiol J. 2012;29:879-885.

17. Roy C, Alam M, Mandal S, Haldar PK, Bhattacharya S, Mukherjee T, et al. Global association between thermophilicity and vancomycin susceptibility in bacteria. Front Microbiol. 2016;7:412.

18. Mondal N, Peketi A, Mapder T, Roy C, Mazumdar A, Chakraborty R, et al. Indus and Nubra Valley hot springs affirm the geomicrobiological specialties of Trans-Himalayan hydrothermal systems. J Earth Syst Sci. 2022;131:12.

19. Wang S, Hou W, Dong H, Jiang H, Huang L, Wu G, et al. Control of temperature on microbial community structure in hot springs of the Tibetan Plateau. PLoS One. 2013;8:e62901.

20. Zhang Y, Wu G, Jiang H, Yang J, She W, Khan I, et al. Abundant and rare microbial biospheres respond differently to environmental and spatial factors in Tibetan hot springs. Front in Microbiol. 2018;9:2096.

21. Das S, Sherpa MT, Najar IN, Thakur N. Prevalence of methanogens in the uncultured Sikkim hot spring solfataric mud archaeal microbiome. Environ Sustain. 2020;3:453-469.

22. Guo L, Wang G, Sheng Y, Sun X, Shi Z, Xu Q, et al. Temperature governs the distribution of hot spring microbial community in three hydrothermal fields, Eastern Tibetan Plateau Geothermal Belt, Western China. Sci Total Environ. 2020;720:137574.

23. Kumar V, Kumar S, Singh D. Metagenomic insights into Himalayan glacial and kettle lake sediments revealed microbial community structure, function, and stress adaptation strategies. Extremophiles. 2022;26:3.

24. Nagar S, Talwar C, Motelica-Heino M, Richnow HH, Shakarad M, Lal R, et al. Microbial Ecology of Sulfur Biogeochemical Cycling at a Mesothermal Hot Spring Atop Northern Himalayas, India. Front Microbiol. 2022;13:848010.

25. Zhang P, Xiong J, Qiao N, Luo S, Yang Q, Li X, et al. High Variation in Protist Diversity and Community Composition in Surface Sediment of Hot Springs in Himalayan Geothermal Belt, China. Microorganisms. 2023;11:674.

26. Roy C, Bakshi U, Rameez MJ, Mandal S, Haldar PK, Pyne P, et al. Phylogenomics of an uncultivated, aerobic and thermophilic, photoheterotrophic member of Chlorobia sheds light into the evolution of the phylum Chlorobi. Comput Biol Chem. 2019;80:206-216.

27. Mondal N, Roy C, Chatterjee S, Sarkar J, Dutta S, Bhattacharya S, et al. Thermal endurance by a hot-spring-dwelling phylogenetic relative of the mesophilic *Paracoccus*. Microbiol Spectr. 2022;10:e01606-22.

28. Steller LH, Nakamura E, Ota T, Sakaguchi C, Sharma M, Van Kranendonk MJ. Boron isotopes in the Puga geothermal system, India, and their implications for the habitat of early life. Astrobiology. 2019;19:1459-1473.

29. Sarkar S, Moitra H, Bhattacharya S, Dagar A, Ray D, Gupta S, et al. Spectroscopic studies on the Puga Hot Spring Deposits, Ladakh, an astrobiological Martian analog site in India. J Geophys Res Planets. 2022;127:e2022JE007299.

30. Campanaro S, Treu L, Kougias PG, Zhu X, Angelidaki I. Taxonomy of anaerobic digestion microbiome reveals biases associated with the applied high throughput sequencing strategies. Sci Rep. 2018;8:1926.

31. Laudadio I, Fulci V, Palone F, Stronati L, Cucchiara S, Carissimi C. Quantitative assessment of shotgun metagenomics and 16S rDNA amplicon sequencing in the study of human gut microbiome. OMICS J Integr Biol. 2018;22:248-254.

32. Brumfield KD, Huq A, Colwell RR, Olds JL, Leddy MB. Microbial resolution of whole genome shotgun and 16S amplicon metagenomic sequencing using publicly available NEON data. PLoS One. 2020;15:e0228899.

33. Durazzi F, Sala C, Castellani G, Manfreda G, Remondini D, De Cesare A. Comparison between 16S rRNA and shotgun sequencing data for the taxonomic characterization of the gut microbiota. Sci Rep. 2021;11:3030.

34. Tessler M, Neumann JS, Afshinnekoo E, Pineda M, Hersch R, Velho LF, et al. Large-scale differences in microbial biodiversity discovery between 16S amplicon and shotgun sequencing. Sci Rep. 2017;7:6589.

35. Peterson D, Bonham KS, Rowland S, Pattanayak CW, Resonance Consortium, Klepac-Ceraj V. Comparative analysis of 16S rRNA gene and metagenome sequencing in pediatric gut microbiomes. Front Microbiol. 2021;12:670336.

36. Takai K, Komatsu T, Horikoshi K. *Hydrogenobacter subterraneus* sp. nov., an extremely thermophilic, heterotrophic bacterium unable to grow on hydrogen gas, from deep subsurface geothermal water. Int J Syst Evol Microbiol. 2001;51:1425-1435.

37. O'Neill AH, Liu Y, Ferrera I, Beveridge TJ, Reysenbach AL. *Sulfurihydrogenibium rodmanii* sp. nov., a sulfur-oxidizing chemolithoautotroph from the Uzon Caldera, Kamchatka Peninsula, Russia, and emended description of the genus *Sulfurihydrogenibium*. Int J Syst Evol Microbiol. 2008;58:1147-1152.

38. Cai J, Wang Y, Liu D, Zeng Y, Xue Y, Ma Y, et al. *Fervidobacterium changbaicum* sp. nov., a novel thermophilic anaerobic bacterium isolated from a hot spring of the Changbai Mountains, China. Int J Syst Evol Microbiol. 2007;57:2333-2336.

39. Chung AP, Rainey FA, Valente M, Nobre MF, da Costa MS. *Thermus igniterrae* sp. nov. and *Thermus antranikianii* sp. nov., two new species from Iceland. Int J Syst Evol Microbiol. 2000;50:209-217.

40. Kashefi K, Holmes DE, Reysenbach AL, Lovley DR. Use of Fe (III) as an electron acceptor to recover previously uncultured hyperthermophiles: isolation and characterization of *Geothermobacterium ferrireducens* gen. nov., sp. nov. Appl Environ Microbiol. 2002;68:1735-1742.

41. Stetter KO, König H, Stackebrandt E. *Pyrodictium* gen. nov., a new genus of submarine disc-shaped sulphur reducing archaebacteria growing optimally at 105°C. Syst Appl Microbiol. 1983;4:535-551.

42. Copeland JJ. Yellowstone thermal myxophyceae. Ann N Y Acad Sci. 1936;36:4-223.

43. Ward DM, Castenholz RW, Miller SR, Whitton B. Cyanobacteria in geothermal habitats. In: Whitton BA (ed). Ecology of cyanobacteria II: their diversity in space and time. Springer Science and Business media, 2012. pp 39-63.

44. Katoh H, Itoh S, Shen JR, Ikeuchi M. Functional analysis of psbV and a novel c-type cytochrome gene psbV2 of the thermophilic cyanobacterium *Thermosynechococcus elongatus* strain BP-1. Plant Cell Physiol. 2001;42:599-607.

45. Komárek J, Johansen JR, Šmarda J, Strunecký O. Phylogeny and taxonomy of *Synechococcus*-like cyanobacteria. Fottea. 2020;20:171-191.

46. Yamaoka T, Satoh K, Katoh S. Photosynthetic activities of a thermophilic blue-green alga. Plant Cell Physiol. 1978;19:943-954.

47. Liang Y, Tang J, Luo Y, Kaczmarek MB, Li X, Daroch M. *Thermosynechococcus* as a thermophilic photosynthetic microbial cell factory for CO_2 utilisation. Bioresour Technol. 2019;278:255-265.

48. Guan TW, Xiao J, Zhao K, Luo XX, Zhang XP, Zhang LL. *Halomonas xinjiangensis* sp. nov., a halotolerant bacterium isolated from a salt lake. Int J Syst Evol Microbiol. 2010;60:349-352.

49. Sun X, Luo P, Li M. *Paracoccus angustae* sp. nov., isolated from soil. Int J Syst Evol Microbiol. 2015;65:3469-3475.

50. Mori K, Suzuki KI. *Thiofaba tepidiphila* gen. nov., sp. nov., a novel obligately chemolithoautotrophic, sulfur-oxidizing bacterium of the Gammaproteobacteria isolated from a hot spring. Int J Syst Evol Microbiol. 2008;58:1885-1891.

51. Chen WM, Huang HW, Chang JS, Han YL, Guo TR, Sheu SY. *Tepidimonas fonticaldi* sp. nov., a slightly thermophilic betaproteobacterium isolated from a hot spring. Int J Syst Evol Microbiol. 2013;63:1810-1816.

52. Meng YC, Liu HC, Zhou YG, Cai M, Kang Y. *Vibrio gangliei* sp. nov., a novel member of Vibrionaceae isolated from sawdust in a pigpen. Int J Syst Evol Microbiol. 2018;68:1969-1974.

53. Kaye JZ, Marquez MC, Ventosa A, Baross JA. *Halomonas neptunia* sp. nov., *Halomonas sulfidaeris* sp. nov., *Halomonas axialensis* sp. nov. and *Halomonas hydrothermalis* sp. nov.: halophilic bacteria isolated from deep-sea hydrothermal-vent environments. Int J Syst Evol Microbiol. 2004;54:499-511.

54. Hasan NA, Grim CJ, Lipp EK, Rivera IN, Chun J, Haley BJ, et al. Deep-sea hydrothermal vent bacteria related to human pathogenic *Vibrio* species. Proc Natl Acad Sci USA. 2015;112:E2813-E2819.

55. Du R, Gao D, Wang Y, Liu L, Cheng J, Liu J, et al. Heterotrophic sulfur oxidation of *Halomonas titanicae* SOB56 and its habitat adaptation to the hydrothermal environment. Front Microbiol. 2022;13:888833.

56. Lipscomb GL, Hahn EM, Crowley AT, Adams MW. Reverse gyrase is essential for microbial growth at 95°C. Extremophiles. 2017;21:603-608.

57. Kampmann M, Stock D. Reverse gyrase has heat-protective DNA chaperone activity independent of supercoiling. Nucleic Acids Res. 2004;32:3537-3545.

58. Murayama N, Shimizu H, Takiguchi S, Baba Y, Amino H, Horiuchi T, et al. Evidence for involvement of *Escherichia coli* genes pmbA, csrA and a previously unrecognized gene tldD, in the control of DNA gyrase by letD (ccdB) of sex factor F. J Mol Biol. 1996;256:483-502.

59. Sengupta S, Nagaraja V. YacG from *Escherichia coli* is a specific endogenous inhibitor of DNA gyrase. Nucleic Acids Res. 2008;36:4310-4316.

60. Smith B, Oliver JD. In situ and in vitro gene expression by *Vibrio vulnificus* during entry into, persistence within, and resuscitation from the viable but nonculturable state. Appl Environ Microbiol. 2006;72:1445-1451.

61. Naskar S, Hohl M, Tassinari M, Low HH. The structure and mechanism of the bacterial type II secretion system. Mol Microbiol. 2021;115:412-424.

62. Liu X, Luo Y, Li Z, Wei G. Functional analysis of a putative type III secretion system in stress adaption by *Mesorhizobium alhagi* CCNWXJ12-2^{T}. Front Microbiol. 2018;9:263.

63. Banerjee G, Quan FS, Mondal AK, Sur S, Banerjee P, Chattopadhyay P. Interrelation between Stress Management and Secretion Systems of *Ralstonia solanacearum*: An In Silico Assessment. Pathogens. 2022;11:730.

64. Souza DP, Oka GU, Alvarez-Martinez CE, Bisson-Filho AW, Dunger G, Hobeika L, et al. Bacterial killing via a type IV secretion system. Nat Commun. 2015;6:6453.

65. Yu KW, Xue P, Fu Y, Yang L. T6SS mediated stress responses for bacterial environmental survival and host adaptation. Int J Mol Sci. 2021;22:478.

66. Hufnagel DA, Evans ML, Greene SE, Pinkner JS, Hultgren SJ, Chapman MR. The catabolite repressor protein-cyclic AMP complex regulates csgD and biofilm formation in uropathogenic *Escherichia coli*. J Bacteriol. 2016;198:3329-3334.

67. Lasica AM, Ksiazek M, Madej M, Potempa J. The type IX secretion system (T9SS): highlights and recent insights into its structure and function. Front Cell Infect Microbiol. 2017;7:215.

68. Mahajan GB, Balachandran L. Sources of antibiotics: Hot springs. Biochem Pharmacol. 2017;134:35-41.

69. Harinarayana T, Azeez KA, Murthy DN, Veeraswamy K, Rao SE, Manoj C, et al. Exploration of geothermal structure in Puga geothermal field, Ladakh Himalayas, India by magnetotelluric studies. J Appl Geophys. 2006;58:280-295.

70. Quan X, Nitta K, Matoba O, Xia P, Awatsuji Y. Phase and fluorescence imaging by combination of digital holographic microscopy and fluorescence microscopy. Opt Rev. 2015 Apr;22:349-53.

71. Absher M. Hemocytometer counting. In Kruse PF, Patterson MK (eds). Tissue culture. Academic Press, 1973. pp 395-397.

72. Li D, Liu CM, Luo R, Sadakane K, Lam TW. MEGAHIT: an ultra-fast single-node solution for large and complex metagenomics assembly via succinct de Bruijn graph. Bioinformatics. 2015;31:1674-1676.

73. Hyatt D, Chen GL, LoCascio PF, Land ML, Larimer FW, Hauser LJ. Prodigal: prokaryotic gene recognition and translation initiation site identification. BMC Bioinformatics. 2010;11:119.

74. Huerta-Cepas J, Szklarczyk D, Heller D, Hernández-Plaza A, Forslund SK, Cook H, et al. eggNOG 5.0: a hierarchical, functionally and phylogenetically annotated orthology resource based on 5090 organisms and 2502 viruses. Nucleic Acids Res. 2019;47:D309-D314.

75. Cantalapiedra CP, Hernández-Plaza A, Letunic I, Bork P, Huerta-Cepas J. eggNOG-mapper v2: functional annotation, orthology assignments, and domain prediction at the metagenomic scale. Mol Biol Evol. 2021;38:5825-5829.

76. Stoddard SF, Smith BJ, Hein R, Roller BR, Schmidt TM. rrn DB: improved tools for interpreting rRNA gene abundance in bacteria and archaea and a new foundation for future development. Nucleic Acids Res. 2015;43:D593-D598.

77. Langmead B, Salzberg SL. Fast gapped-read alignment with Bowtie 2. Nat Methods. 2012;9:357-359.

78. Quast C, Pruesse E, Yilmaz P, Gerken J, Schweer T, Yarza P, et al. The SILVA ribosomal RNA gene database project: improved data processing and web-based tools. Nucleic Acids Res. 2013;41:D590-D596.

79. Seemann T. barrnap 0.9: rapid ribosomal RNA prediction. 2018. https://github.com/tseemann/barrnap

80. Pruesse E, Peplies J, Glöckner FO. SINA: accurate high-throughput multiple sequence alignment of ribosomal RNA genes. Bioinformatics. 2012;28:1823-1829.

81. Kang DD, Froula J, Egan R, Wang Z. MetaBAT, an efficient tool for accurately reconstructing single genomes from complex microbial communities. PeerJ. 2015;3:e1165.

82. Wu YW, Simmons BA, Singer SW. MaxBin 2.0: an automated binning algorithm to recover genomes from multiple metagenomic datasets. Bioinformatics. 2016;32:605-607.

83. Alneberg J, Bjarnason BS, De Bruijn I, Schirmer M, Quick J, Ijaz UZ, et al. Binning metagenomic contigs by coverage and composition. Nat Methods. 2014;11:1144-1146.

84. Sieber CM, Probst AJ, Sharrar A, Thomas BC, Hess M, Tringe SG, et al. Recovery of genomes from metagenomes via a dereplication, aggregation and scoring strategy. Nat Microbiol. 2018;3:836-843.

85. Parks DH, Imelfort M, Skennerton CT, Hugenholtz P, Tyson GW. CheckM: assessing the quality of microbial genomes recovered from isolates, single cells, and metagenomes. Genome Res. 2015;25:1043-1055.

86. Chaumeil PA, Mussig AJ, Hugenholtz P, Parks DH. GTDB-Tk: a toolkit to classify genomes with the Genome Taxonomy Database. Bioinformatics. 2020;36:1925-1927.

87. Aziz RK, Bartels D, Best AA, DeJongh M, Disz T, Edwards RA, et al. The RAST Server: rapid annotations using subsystems technology. BMC Genom. 2008;9:75.

88. Meier-Kolthoff JP, Carbasse JS, Peinado-Olarte RL, Göker M. TYGS and LPSN: a database tandem for fast and reliable genome-based classification and nomenclature of prokaryotes. Nucleic Acids Res. 2022;50:D801-D807.

89. Yoon SH, Ha SM, Lim J, Kwon S, Chun J. A large-scale evaluation of algorithms to calculate average nucleotide identity. Antonie Van Leeuwenhoek. 2017;110:1281-1286.

90. Na SI, Kim YO, Yoon SH, Ha SM, Baek I, Chun J. UBCG: up-to-date bacterial core gene set and pipeline for phylogenomic tree reconstruction. J Microbiology. 2018;56:280-285.

91. Darriba D, Posada D, Kozlov AM, Stamatakis A, Morel B, Flouri T. ModelTest-NG: a new and scalable tool for the selection of DNA and protein evolutionary models. Mol Biol Evol. 2020; *37*:291-294.

92. Stamatakis A. RAxML version 8: a tool for phylogenetic analysis and post-analysis of large phylogenies. Bioinformatics. 2014; 30:1312-1313.

93. Letunic I, Bork P. Interactive Tree Of Life (iTOL) v4: recent updates and new developments. Nucleic Acids Res. 2019;47:W256-W259.

94. Ghosh W, Roy C, Roy R, Nilawe P, Mukherjee A, Haldar PK, et al. Resilience and receptivity worked in tandem to sustain a geothermal mat community amidst erratic environmental conditions. Sci Rep. 2015;5:12179.

95. Edgar RC. UPARSE: highly accurate OTU sequences from microbial amplicon reads. Nat Methods. 2013;10:996-998.

Legend of Figures

Fig. 1. Representative picture of the fluorescence microscopic fields based on which microbial cell density was calculated in the vent-water sample of Lotus Pond: (**A**) sample stained with DAPI, (**B**) sample stained with FDA, (**C**) sample stained with PI. Scale bars in all the three micrographs indicate 50 µm length.

Fig. 2. Taxonomic distribution of (**A**) the CDSs identified in the assembled whole metagenome of Lotus Pond, and (**B**) the metagenomic reads which corresponded to 16S rRNA genes (actual CDS count or metagenomic read count recorded for each taxon is given in parenthesis). In (**A**) “minor phyla” included the following: Acidobacteria, Chlamydiae, Chlorobi, Deferribacteres, Fusobacteria, Gemmatimonadetes, Nitrospirae, Planctomycetes, Spirochaetes, Synergistetes, Tenericutes, Thermomicrobia and Verrucomicrobia. In (**B**) “other phyla”, also marginal in representation, included the following: Cyanobacteria, Thermotogae, Bacteroidetes, Chloroflexi, Actinobacteria, Armatimonadetes and Synergistetes.

Fig. 3. Phylogenetic tree (number of bootstrap tests carried out = 10000), based on 92 universal bacterial core genes, showing the evolutionary relationships among the 14 bacterial MAGs reconstructed from the Lotus Pond vent-water metagenome and their closest relatives identified based on dDDH and/or rRNA gene sequence relationships. Scale bar denotes a distance equivalent to 10% nucleotide substitution. In the phylogeny reconstructed, nucleotide substitutions were interpreted using the generalized time-reversible model, which considers the proportion of invariable sites and/or the rate of variation across the sites.

Table 1. Key features of the population genome bins (MAGs) constructed from the assembled metagenome of Lotus Pond's vent-water.

Name of the population genome bin obtained (genome accession number)	% of quality-filtered metagenomic read-pairs matching sequences of the MAG concordantly	No. of contigs	Genome size (nucleotides)	G+C content (%)	Completeness (%)	Contamination (%)	Number of ORFs (genes) / CDSs detected in the MAG
LotusPond_MAG_Unclassified_Aquificaceae (JARJNB000000000)	55.92	131	1489711	43.32	95.12	0.61	1754 / 1707
LotusPond_MAG_Sulfurihydrogenibium_azorense (JARJNA000000000)	3.48	47	1516769	32.77	98.98	0.00	1680 / 1639
LotusPond_MAG_Halomonas_sp. (JARJMQ000000000)	2.65	97	3349510	60.21	99.46	0.94	3245 / 3176
LotusPond_MAG_Unclassified_Desulfurococcales (JARJMZ000000000)	1.60	37	1553981	49.38	99.63	0.00	1621 / 1559
LotusPond_MAG_Vibrio_metschnikovii (JARJMP000000000)	1.54	249	3487509	44.28	94.07	1.85	3222 / 3172
LotusPond_MAG_Thermus_sp. (JARJMW000000000)	1.01	372	1887946	62.80	70.34	4.24	2206 / 2157
LotusPond_MAG_Tepidimonas_sp. (JARJMT000000000)	0.46	200	2150705	66.30	94.16	1.29	2200 / 2155
LotusPond_MAG_Thermosynechococcus_sp. (JARJMS000000000)	0.35	104	2328058	52.52	97.05	0.12	2367 / 2319
LotusPond_MAG_Tepidimonas_taiwanensis (JARJMR000000000)	0.28	245	2568138	69.51	90.53	3.56	2567 / 2525
LotusPond_MAG_Fervidobacterium_sp. (JARJMY000000000)	0.24	293	1525481	39.93	70.18	0.88	1639 / 1611
LotusPond_MAG_Paracoccus_sp._1 (JARJMU000000000)	0.17	528	2138329	62.94	51.22	15.08	2383 / 2345
LotusPond_MAG_Unclassified_Bacteria (JARJMV000000000)	0.11	335	2025372	61.84	81.86	0.31	2082 / 2039
LotusPond_MAG_Unclassified_Chromatiales (JARJMX000000000)	0.10	214	1644354	62.57	91.04	2.01	1796 / 1758
LotusPond_MAG_Unclassified_Thermodesulfobacteriaceae (JARJND000000000)	0.07	114	439694	36.23	30.15	0.31	477 / 467
LotusPond_MAG_Paracoccus_sp._2 (JARJNC000000000)	0.06	284	1087115	64.14	34.31	1.10	1214 / 1201

Table 2. Bacterial genera that were detected in the present exploration of the Lotus Pond vent-water as well as in one or more previous studies of the same habitat using 16S rRNA gene sequence analysis.

Phylum to which the genera belonged	Names of the genera[1,2]	Maximum temperature for Laboratory-growth[3] (°C)	Sampling date of the previous study in which the genus was also identified	
			23 July, 2013 [17]	20 October, 2014 [10]
Actinobacteria	***Brevibacterium***	42	+	+
	Corynebacterium	42	+	+
	Mycobacterium	43	-	+
	Nocardioides	37	-	+
	Ornithinimicrobium	50	+	-
	Rothia	38	+	-
Armatimonadetes	Gp5	-	-	+
	Gp7	-	-	+
Aquificae	***Hydrogenobacter***	85	+	+
	Sulfurihydrogenibium	80	+	+
Bacteroidetes	***Chryseobacterium***	37	+	+
	Cloacibacterium	40	+	+
	Pedobacter	35	-	+
	Porphyromonas	37	+	-
	Prevotella	45	+	-
Chloroflexi	***Chloroflexus***	59	+	+
Cyanobacteria	**GpXIII**	-	-	+
	GpIV	-	-	+
Deinococcus-Thermus	***Thermus***	80	+	+
	Truepera	50	+	+
Dictyoglomi	***Dictyoglomus***	80	-	+
Firmicutes	***Anoxybacillus***	70	+	+
	Bacillus	70	+	+
	Chryseomicrobium	45	+	-
	Enterococcus	45	+	-
	Exiguobacterium	49	+	+
	Gemella	37	-	+
	Lactococcus	40	+	-
	Lysinibacillus	45	-	+
	Planococcus	42	+	+
	Sporolactobacillaceae _incertae_sedis	-	-	+
	Staphylococcus	40	+	+
	Streptococcus	45	+	+
Alphaproteobacteria	***Azospirillum***	37	+	+
	Bradyrhizobium	37	+	+
	Brevundimonas	42	+	+
	Paracoccus	45	+	+
	Sphingobium	37	-	+
	Sphingomonas	45	+	+
	Sulfitobacter	40	+	+
Betaproteobacteria	***Achromobacter***	42	+	+
	Acidovorax	37	+	+
	Burkholderia	37	+	+
	Comamonas	44	-	+
	Delftia	40	-	+

	Herbaspirillum	45	+	-
	Pelomonas	37	+	+
	Ralstonia	41	+	+
	Tepidimonas	60	+	+
Gammaproteobacteria	***Aeromonas***	41	+	+
	Acinetobacter	37	+	+
	Buttiauxella	42	-	+
	Enhydrobacter	41	+	+
	Escherichia/Shigella	37	-	+
	Halomonas	50	+	+
	Klebsiella	37	-	+
	Marinobacter	50	+	+
	Pseudomonas	42	-	+
	Psychrobacter	38	+	+
	Rheinheimera	35	-	+
	Serratia	35	+	-
	Shewanella	30	+	-
	Stenotrophomonas	42	+	+
	Thiofaba	51	+	+
	Thiovirga	34	+	-
Thermotogae	***Fervidobacterium***	90	+	+

[1] Genera detected in the present PCR-amplified 16S rRNA gene sequence analysis are indicated by bold fonts.

[2] Names of the genera that were detected in the present annotation of metagenomic reads corresponding to 16S rRNA genes are underscored.

[3] Full references concerning the maximum temperatures for laboratory-growth of all the above genera have been cited in relation to Tables S3 and S4, within the Supplementary Information file.

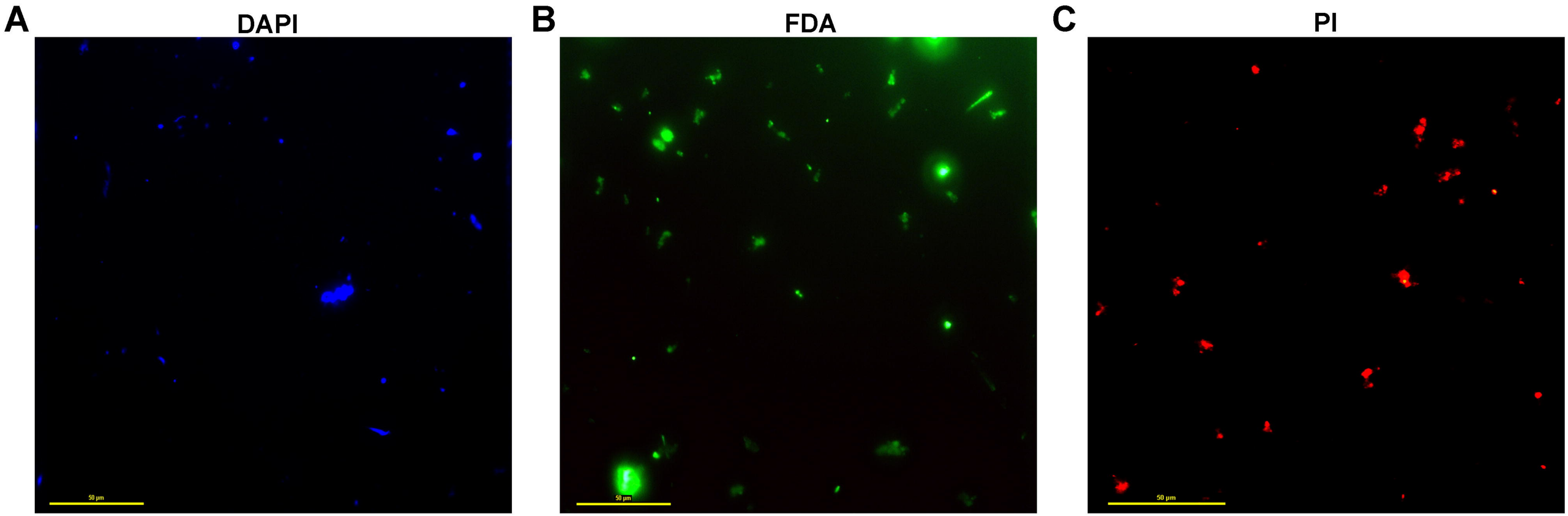
A
DAPI
50 µm
B
FDA
50 µm
C
PI
50 µm

A

Taxonomic classification of bacterial CDSs identified in the assembled metagenome

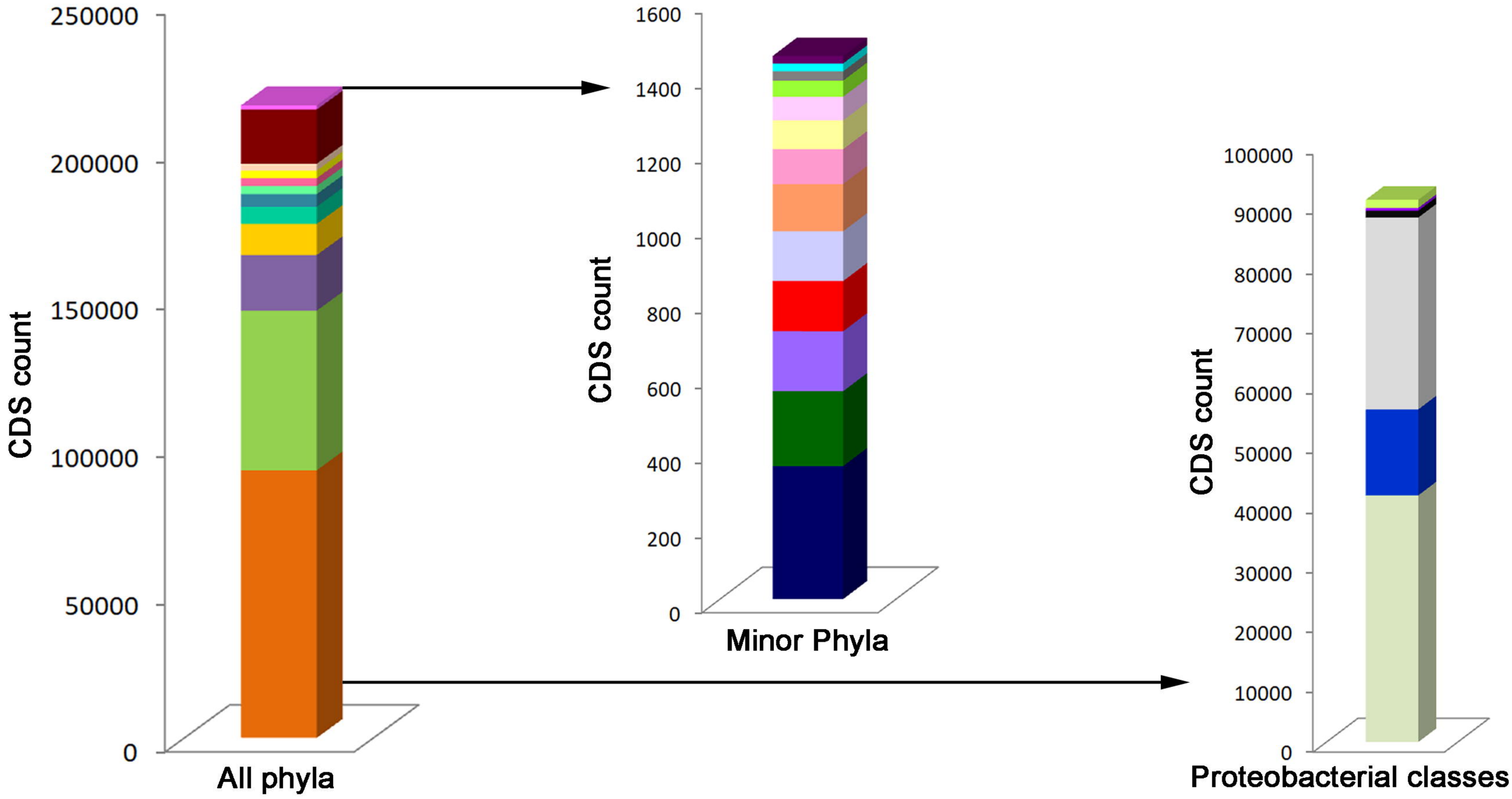

Proteobacteria (90793)
Aquificae (54151)
Firmicutes (18872)
Deinococcus-Thermus (10591)
Cyanobacteria (5827)
Chloroflexi (4254)
Bacteroidetes (2753)
Thermotogae (2671)
Thermodesulfobacteria (2547)
Actinobacteria (2357)
Unclassified Bacteria (18386)
Minor phyla (1450)
Planctomycetes (355)
Synergistetes (200)
Verrucomicrobia (160)
Acidobacteria (134)
Fusobacteria (133)
Nitrospirae (126)
Chlorobi (93)
Spirochaetes (77)
Thermomicrobia (63)
Deferribacteres (43)
Tenericutes (25)
Gemmatimonadetes (21)
Chlamydiae (20)
Alphaproteobacteria (41306)
Betaproteobacteria (14394)
Gammaproteobacteria (32111)
Deltaproteobacteria (1145)
Epsilonproteobacteria (466)
Other Proteobacteria (1371)

B

Taxonomic classification of metagenomic reads which corresponded to bacterial 16S rRNA genes

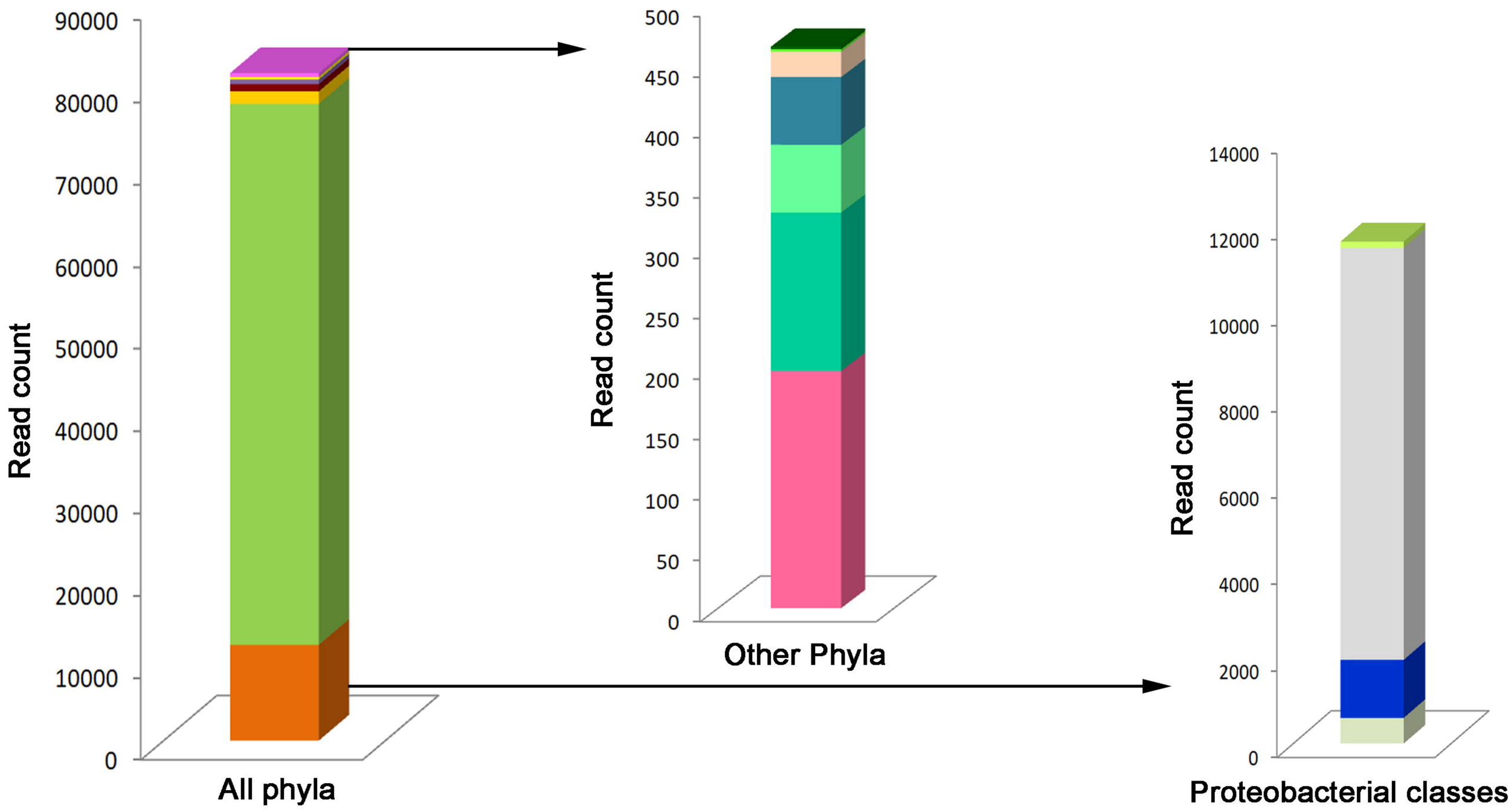

Proteobacteria (11639)
Aquificae (65853)
Deinococcus-Thermus (1517)
Unclassified Bacteria (875)
Firmicutes (567)
Thermodesulfobacteria (308)
Other Phyla (464)
Thermotogae (196)
Cyanobacteria (131)
Bacteroidetes (56)
Chloroflexi (56)
Actinobacteria (21)
Armatimonadetes (2)
Synergistetes (2)
Alphaproteobacteria (595)
Betaproteobacteria (1345)
Gammaproteobacteria (9553)
Other Proteobacteria (146)

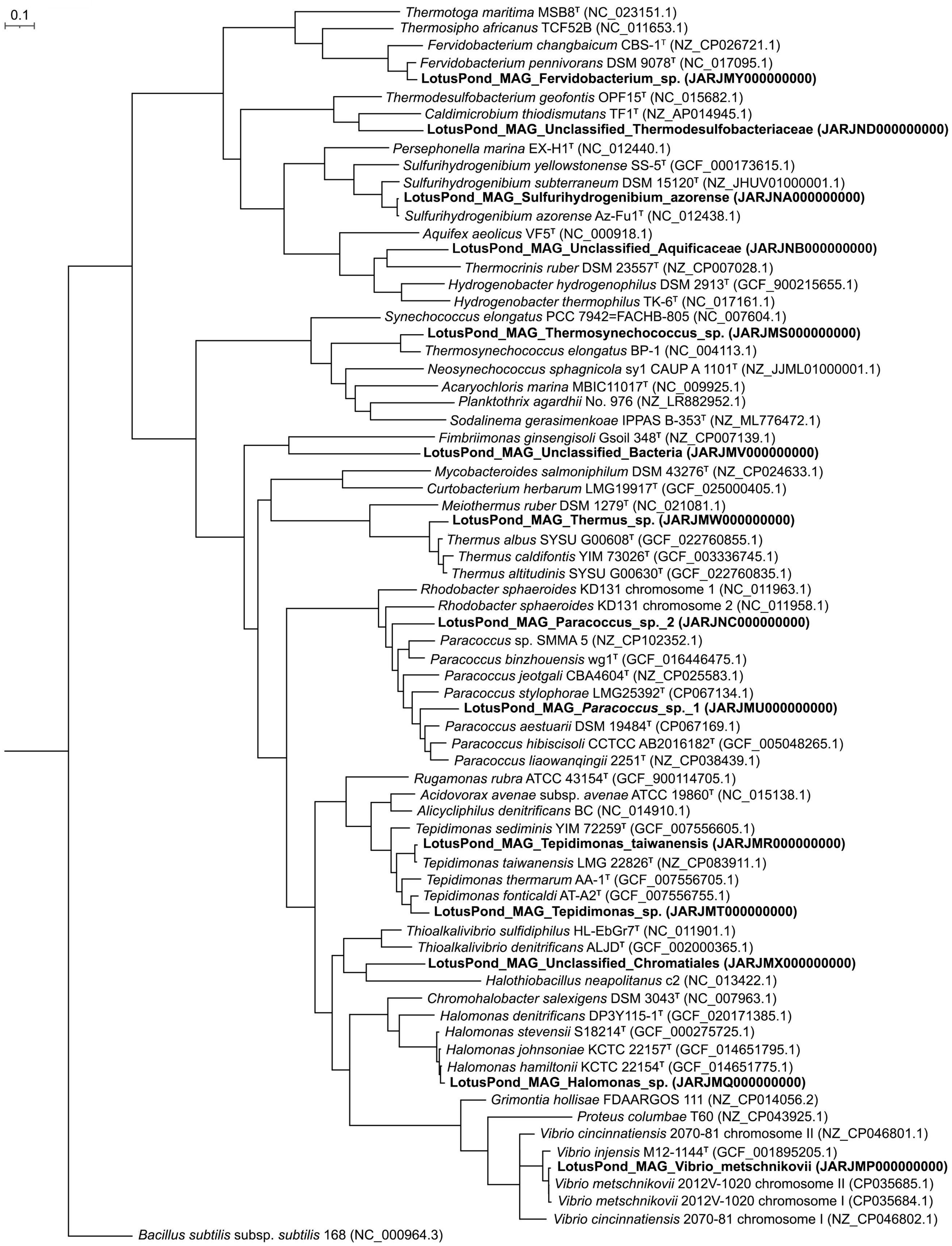
0.1
Thermotoga maritima MSB8T (NC_023151.1)
Thermosipho africanus TCF52B (NC_011653.1)
Fervidobacterium changbaicum CBS-1T (NZ_CP026721.1)
Fervidobacterium pennivorans DSM 9078T (NC_017095.1)
LotusPond_MAG_Fervidobacterium_sp. (JARJMY000000000)
Thermodesulfobacterium geofontis OPF15T (NC_015682.1)
Caldimicrobium thiodismutans TF1T (NZ_AP014945.1)
LotusPond_MAG_Unclassified_Thermodesulfobacteriaceae (JARJND000000000)
Persephonella marina EX-H1T (NC_012440.1)
Sulfurihydrogenibium yellowstonense SS-5T (GCF_000173615.1)
Sulfurihydrogenibium subterraneum DSM 15120T (NZ_JHUV01000001.1)
LotusPond_MAG_Sulfurihydrogenibium_azorense (JARJNA000000000)
Sulfurihydrogenibium azorense Az-Fu1T (NC_012438.1)
Aquifex aeolicus VF5T (NC_000918.1)
LotusPond_MAG_Unclassified_Aquificaceae (JARJNB000000000)
Thermocrinis ruber DSM 23557T (NZ_CP007028.1)
Hydrogenobacter hydrogenophilus DSM 2913T (GCF_900215655.1)
Hydrogenobacter thermophilus TK-6T (NC_017161.1)
Synechococcus elongatus PCC 7942=FACHB-805 (NC_007604.1)
LotusPond_MAG_Thermosynechococcus_sp. (JARJMS000000000)
Thermosynechococcus elongatus BP-1 (NC_004113.1)
Neosynechococcus sphagnicola sy1 CAUP A 1101T (NZ_JJML01000001.1)
Acaryochloris marina MBIC11017T (NC_009925.1)
Planktothrix agardhii No. 976 (NZ_LR882952.1)
Sodalinema gerasimenkoae IPPAS B-353T (NZ_ML776472.1)
Fimbriimonas ginsengisoli Gsoil 348T (NZ_CP007139.1)
LotusPond_MAG_Unclassified_Bacteria (JARJMV000000000)
Mycobacteroides salmoniphilum DSM 43276T (NZ_CP024633.1)
Curtobacterium herbarum LMG19917T (GCF_025000405.1)
Meiothermus ruber DSM 1279T (NC_021081.1)
LotusPond_MAG_Thermus_sp. (JARJMW000000000)
Thermus albus SYSU G00608T (GCF_022760855.1)
Thermus caldifontis YIM 73026T (GCF_003336745.1)
Thermus altitudinis SYSU G00630T (GCF_022760835.1)
Rhodobacter sphaeroides KD131 chromosome 1 (NC_011963.1)
Rhodobacter sphaeroides KD131 chromosome 2 (NC_011958.1)
LotusPond_MAG_Paracoccus_sp._2 (JARJNC000000000)
Paracoccus sp. SMMA 5 (NZ_CP102352.1)
Paracoccus binzhouensis wg1T (GCF_016446475.1)
Paracoccus jeotgali CBA4604T (NZ_CP025583.1)
Paracoccus stylophorae LMG25392T (CP067134.1)
LotusPond_MAG_Paracoccus_sp._1 (JARJMU000000000)
Paracoccus aestuarii DSM 19484T (CP067169.1)
Paracoccus hibiscisoli CCTCC AB2016182T (GCF_005048265.1)
Paracoccus liaowanqingii 2251T (NZ_CP038439.1)
Rugamonas rubra ATCC 43154T (GCF_900114705.1)
Acidovorax avenae subsp. avenae ATCC 19860T (NC_015138.1)
Alicycliphilus denitrificans BC (NC_014910.1)
Tepidimonas sediminis YIM 72259T (GCF_007556605.1)
LotusPond_MAG_Tepidimonas_taiwanensis (JARJMR000000000)
Tepidimonas taiwanensis LMG 22826T (NZ_CP083911.1)
Tepidimonas thermarum AA-1T (GCF_007556705.1)
Tepidimonas fonticaldi AT-A2T (GCF_007556755.1)
LotusPond_MAG_Tepidimonas_sp. (JARJMT000000000)
Thioalkalivibrio sulfidiphilus HL-EbGr7T (NC_011901.1)
Thioalkalivibrio denitrificans ALJDT (GCF_002000365.1)
LotusPond_MAG_Unclassified_Chromatiales (JARJMX000000000)
Halothiobacillus neapolitanus c2 (NC_013422.1)
Chromohalobacter salexigens DSM 3043T (NC_007963.1)
Halomonas denitrificans DP3Y115-1T (GCF_020171385.1)
Halomonas stevensii S18214T (GCF_000275725.1)
Halomonas johnsoniae KCTC 22157T (GCF_014651795.1)
Halomonas hamiltonii KCTC 22154T (GCF_014651775.1)
LotusPond_MAG_Halomonas_sp. (JARJMQ000000000)
Grimontia hollisae FDAARGOS 111 (NZ_CP014056.2)
Proteus columbae T60 (NZ_CP043925.1)
Vibrio cincinnatiensis 2070-81 chromosome II (NZ_CP046801.1)
Vibrio injensis M12-1144T (GCF_001895205.1)
LotusPond_MAG_Vibrio_metschnikovii (JARJMP000000000)
Vibrio metschnikovii 2012V-1020 chromosome II (CP035685.1)
Vibrio metschnikovii 2012V-1020 chromosome I (CP035684.1)
Vibrio cincinnatiensis 2070-81 chromosome I (NZ_CP046802.1)
Bacillus subtilis subsp. subtilis 168 (NC_000964.3)